International Information and Engineering Technology Association
Advancing the World of Information and Engineering

Revue des Composites et des Matériaux Avancés-Journal of Composite and Advanced Materials
Vol. 35, No. 6, December, 2025, pp. 1055-1061
Journal homepage: http://iieta.org/journals/rcma

Ferrite Nanocomposites: Characteristics of Optical and Microwave Performance

Araa H. Hadi[1*], Sameer H. Al-Nesrawy[2]

[1] College of Biotechnology, Al-Qasim Green University, Qasim 51013, Iraq
[2] Department of Physics, College of Education for Pure Sciences, University of Babylon, Hilla 51002, Iraq

Corresponding Author Email: edu222.araa.hasan@student.uobabylon.edu.iq

https://doi.org/10.18280/rcma.350605

Received: 1 November 2025
Revised: 7 December 2025
Accepted: 23 December 2025
Available online: 31 December 2025

Keywords:
nanocomposites, ferrite, field electron-SEM, ultraviolet rays (UV), FTIR, microwave, PMMA, PEO

ABSTRACT

In this work, we investigated the effect of ferrite addition on two polymers (PEO/PMMA) with different weight percentages (1.2, 2.4, and 3.6 wt%). The solution casting technique was used to fabricate the samples, The nanocomposites were studied to further investigate their composition, structure, and insulating properties (PEO/PMMA-Co-Ni-Cr Fe_2O_4). Optical micrographs show an additional distribution of nPs, and the mixture was homogeneous; the Co-Ni-Cr Fe_2O_4 nanoparticles were found in a continuous and ordered structure. Within the lattice, a polymer was present at a concentration of 6 wt%. The spectra exhibited variations in band position and intensity, indicating significant chemical interaction between the polymer and the nanoparticles. Experimental results show that with increasing concentration of (PEO/PMMA-Co-Ni-Cr Fe_2O_4) nanocomposites, their dielectric loss, insulating constant, and dielectric loss increase, while the ferrite nanomaterial decreases, with increasing electric field repetition rate. On the other hand, the AC electrical conductivity increases. The nanoparticles increase in both frequency and concentration. The (PEO/PMMA-Co-Ni-Cr Fe_2O_4) nanostructures may be used to develop new nanocomposite films for microwave absorption applications.

1. INTRODUCTION

The field of applied science known as "nanotechnology" investigates the issue of atomic and molecular-level matter size control. The creation of materials or devices that are 100 nanometers or smaller is the focus of nanotechnology, which is primarily concerned with structures that are that small [1]. Several sectors, like as the automotive, electronics, and systems industries, have benefited from the new methods and trade prospects made possible by nanotechnology's production and nanocomposite applications. Many people believe that nanotechnology will bring about a new era in manufacturing [2]. Ferrites are very hard and brittle ceramic materials that have a dark grey or black appearance. Because of their ferromagnetic behavior, ferrites are categorized as magnetic materials and have a variety of uses [3]. Their structural features can distinguish three types of permanent magnetism: one of the features of magnetic materials (hard ferrite, garnet ferrite, and soft ferrite) [4].

Novel delivery systems have been developed because of developments in the science of polymers. New polymers have been incorporated, leading to the creation of polymers with distinctive properties. In addition to their chemical makeup, the properties of polymeric materials for a particular type of polymer also depend on their molecular weight and the roles that the chain of polymer salts plays in providing useful complexes [5]. New kinds of polymer-filled particles, ranging in size from nanometers to micrometers, are known as polymer nanocomposites [6]. In a nanoscale area, organic polymers and inorganic nanoparticles combine to form nanocomposite polymers [7, 8].

Among the most well-known and ancient polymers is poly(methyl methacrylate) (PMMA). Its versatile usage and appealing physical and visual characteristics make it an important and fascinating polymer. There are a number of intriguing biological characteristics of this polymer. PMMA is an inert polymer that has excellent mechanical strength, low weight, chemical resistance, and transparency [9, 10]. Its refractive index, which may vary from 1.3 to 1.7, further enhances its optical properties and makes it a popular alternative to inorganic glass [9]. A thermoplastic material that is resistant to weathering and corrosion, has excellent hardness and tensile strength, is very rigid, is colorless, and transmits light almost without loss in the (360-1000 nm) wavelength range. It also has sound insulating qualities. It is possible to alter PMMA physically or chemically to make it less brittle and more resistant to chemicals, two of its drawbacks. Hydrophobic (ethylene) and hydrophilic (carbonyl) groups are present in every unit of PMMA. Because it is an insulator polymer, PMMA has many more potential uses. The need to create conducting materials with balanced features, such as high conductivity and acceptable mechanical qualities, has, nevertheless, maintained a long-term focus on synthesizing these materials primarily from PMMA [11]. Also, additional conducting polymers may be physically mixed with PMMA or co-polymerized chemically to create a novel material with synergistic qualities [12].

Polymerization of methyl methacrylate yields PMMA. Due to its extensive usage in the automotive sector, PMMA has surpassed all other methacrylate polymers in terms of usage [13]. With a molecular weight ranging from 600,000 to 4,000,000 g/mol, polyethylene oxide is a nonionic homopolymer of ethylene oxide. Because of its polarity, it may combine with various solvents to create a broad variety of composites. A range of grades is available for this white to off-white powder, each corresponding to a distinct profile of the viscosity of an aqueous isopropyl alcohol solution. It might include an appropriate antioxidant. The environmental friendliness, abundance, cheap cost, and lack of toxicity of polyethylene oxide were the deciding factors in its selection [10, 14].

2. EXPERIMENTAL WORK

Ferrite materials (Co-Ni-Cr Fe_2O_4) were synthesized using the casting method. 75 wt% PMMA and 25 wt% polyethylene oxide (PEO) were added to 100 ml of chloroform. The polymers were mixed for half an hour without heating using a magnetic stirrer to create a uniform solution. The thickness could be measured using a micrometer, reaching a thickness of 10 cm [15]. Different concentrations of polymer materials (1.2, 2.4, and 3.6 wt%) could be added to produce ferrite nanomaterials. The solution container was a Petri dish. Drying took five days at room temperature. The formation of polymer nanocomposites was determined as a function of temperature. The analysis was performed by removing the nanoparticles from Petri dishes made of PEO/PMMA (Co-Ni-Cr Fe_2O_4). Utilizing a double-beam spectrophotometer (Shimadzu, UV-1800 A) operating between the 250 to 850 nm wavelength range, this optical property of nanocomposite films was investigated. Using a 10× magnification optical microscope of the Olympus-type Nikon-73346, the samples were examined at various concentrations. Cu, Ni, Cr, and Fe_2O_4. An electron microscope of the type Vertex 5600LV, manufactured by Bruker Nano GmbH, a German business, is used to analyze the films of nanocomposites [16]. This is seen in Figure 1 below:

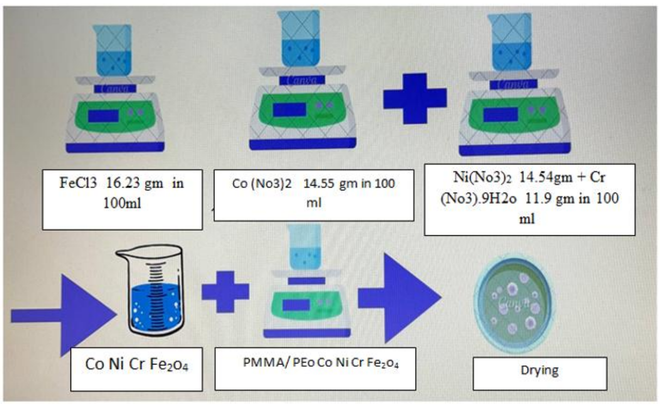

Figure 1. The diagram explaining the steps for preparing the sample

The formula for absorbance (A) is given below [17].

$$A = IA/Io \qquad (1)$$

where, IA is the absorbed light intensity by the material and I_o is the incident intensity of light. Transmittance (T) is computed as Eq. (2) [18]:

$$T = \exp\,[-2.303A] \qquad (2)$$

The dielectric constant is categorized into Two Real (εr) and imaginary (εim) parts. which are given by the following equations [19]:

$$\varepsilon r = n2 - k2 \qquad (3)$$

$$\varepsilon im = 2nk \qquad (4)$$

The optical conductivity (σ) is obtained by using the relation [20]:

$$\sigma = \alpha nc/4\pi \qquad (5)$$

where, c is the velocity of light, n is the refractive index and a is the absorption coefficient.

3. SECTION HEADINGS

Figure 2 shows the relationship between wavelength and absorbance of (Co-Ni-Cr Fe_2O_4) nanocomposites. The figure clearly demonstrates that film absorbance is at its peak at 250 nm, close to the fundamental absorption edge, and gradually decreases with increasing wavelength. In the visible and near-infrared spectrums, film absorbance is typically modest. This performance may be described in this way. The incoming photon has sufficient energy to interact with atoms and is transmitted as its wavelength decreases, approaching the basic absorption edge. As the input photon's wavelength decreases, it interacts with the material, leading to a rise in absorbance [21, 22].

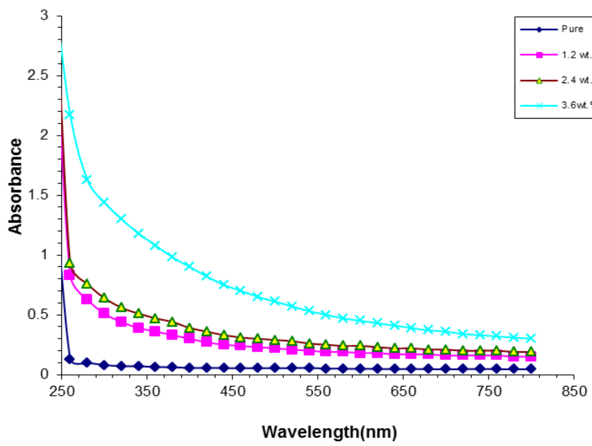

Figure 2. Absorbance spectra for (PEO/PMMA-Co-Ni-Cr Fe_2O_4) nanocomposites films sintering at 1200°C with different ferrite

Figure 3 shows the optical transmittance spectra of (PEO/PMMA-Co-Ni-Cr Fe_2O_4) nanocomposites as a function of incident wavelength. The graph clearly shows that the transmittance decreases with increasing concentration [22].

The absorption coefficient (α) of the materials used nowadays is determined by Eq. (6) [22]:

$$\alpha = (2.303 \times A) / d \qquad (6)$$

where, d is the thickness of the film and A is the absorbance.

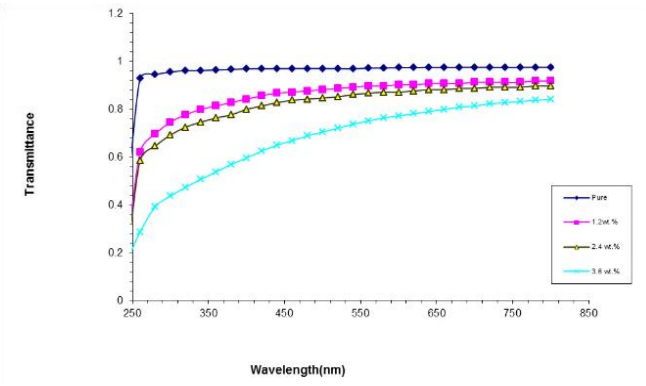

Figure 3. Transmittance spectra for (PEO/PMMA-Co-Ni-Cr Fe_2O_4) nanocomposites films sintering 1200°C with different ferrite ratios

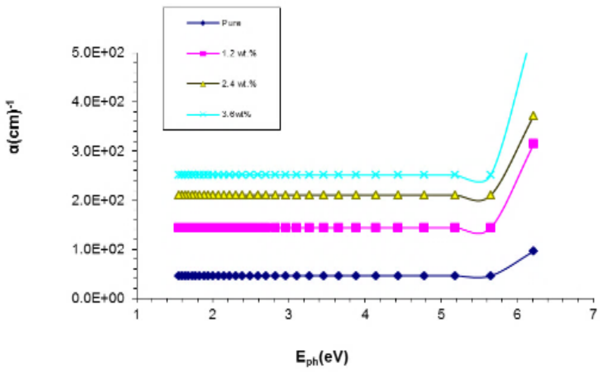

Figure 4. Absorption coefficient for (PEo/PMMA-Co-Ni-Cr Fe_2O_4) nanocomposites films 1200°C with different ferrite ratios

It is dependent on optical transmission, reflection, and film thickness.

The absorption coefficient increased with increasing concentration, as seen in Figure 4. Even when the photon energy (α) increased, the value stayed high and kept going up. In the tested frequency range, an absorption coefficient below 10^4 cm^{-1} indicates that there is an indirect energy band gap in the nanocomposites [23, 24].

The relationship is used to calculate the indirect transition [25]:

$$\alpha h\upsilon = B(h\upsilon - Eg)\ r \qquad (7)$$

where, r = 2 for an allowed indirect transition, r = 3 for a forbidden indirect transition, Eg is the optical band gap, B is constant, and hυ is the incident photon energy (Figures 5 and 6).

With the creation of additional levels in the band gap, the indirect energy gap decreases as the ferrite concentration increases, as shown in Figure 5 for prohibited and permitted indirect energy gaps, respectively.

The extinction coefficient, (k) obtained from the relation [26]:

$$k = \alpha\lambda/4\pi \qquad (8)$$

where, λ is the wavelength and α is the coefficient of absorption.

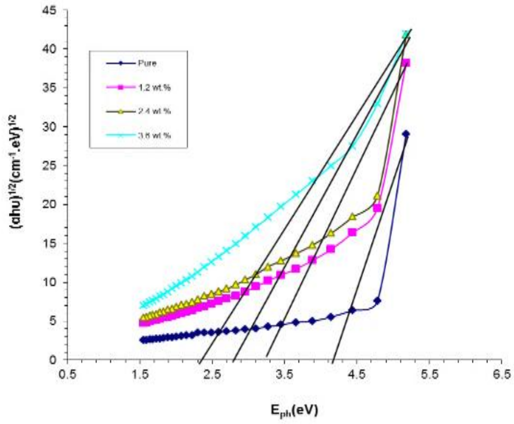

Figure 5. Allowed indirect energy gap for (PEO/PMMA-Co-Ni-Cr Fe_2O_4) nanocomposites films 1200°C with different ferrite ratios

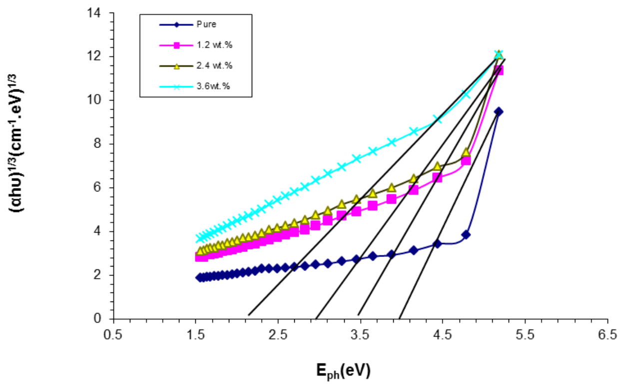

Figure 6. Forbidden indirect energy gap for (PEO/PMMA-Co-Ni-Cr Fe_2O_4) nanocomposites films 1200°C with different ferrite ratios

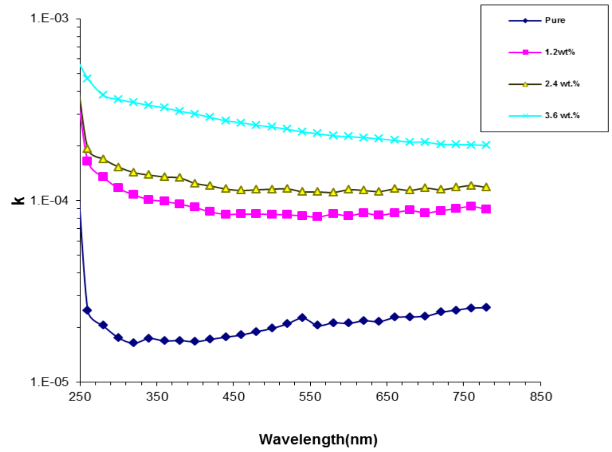

Figure 7. Extinction coefficient for (PEO/PMMA-Co-Ni-Cr Fe_2O_4) nanocomposites films 1200°C with different ferrite ratios

Figure 7 shows the variation of the extinction coefficient of (PEO/PMMA-Co-Ni-Cr Fe_2O_4) nanocomposites with photon energy, this figure shows that when the ferrite concentration rises, the extinction coefficient rises as well [27].

The index of refractive (n) is calculated from Eq. (9) [28]:

$$n = \sqrt{\frac{4R - K^2}{(R-1)^2}} - \frac{R+1}{R-1} \tag{9}$$

where, k is the coefficient of extinction and R is the reflectance.

As a function of wavelength, Figure 8 displays the change index of nanocomposite films of (PEO/PMMA-Co-Ni-Cr Fe_2O_4) with varying ferrite concentrations. The chart clearly demonstrates that the refractive index rises in direct proportion to the ferrite w t%. Reason being, the density of the films made of nanocomposite materials rises [29].

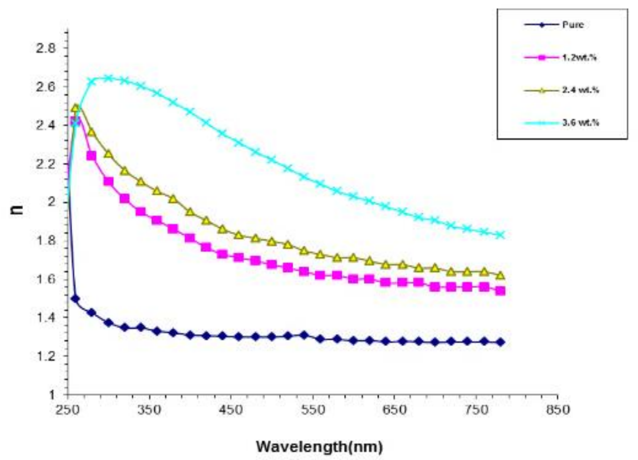

Figure 8. Refractive index for (PEO/PMMA-Co-Ni-Cr Fe_2O_4) nanocomposites films 1200°C with different ferrite ratios

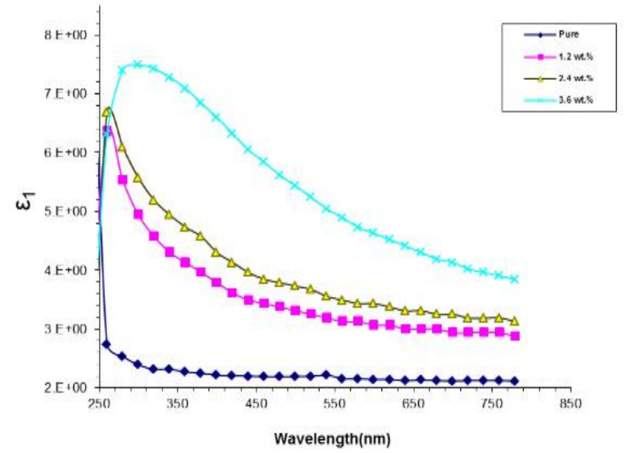

Figure 9. Real dielectric constant for (PEO/PMMA-Co-Ni-Cr Fe_2O_4) nanocomposites films 1200°C with different ferrite ratios

The influence of the samples' real and imaginary portions on photon energy is seen in Figures 8-10, respectively. Given that it is mostly affected by n_2, it follows that ε_1 is bigger than ε_2. This is because the actual component of the dielectric constant diminishes with increasing concentrations of ferrite nanoparticles in PEO/PMMA [30, 31].

The relationship can be used to determine the optical conductivity (σ) [32]:

$$\sigma op = \alpha n c / 4\pi \tag{10}$$

where, α is the absorption coefficient, c is the velocity of light, and n is the refractive index.

Figure 11 shows the relationship between the optical conductivity and wavelength in (Co-Ni-Cr Fe_2O_4) nanocomposites, which may be represented by a film made of (PEO/PMMA-Co-Ni-Cr Fe_2O_4). The optical conductivity of the increases with increasing percentages of the, according to the research [33]. Because of these additional levels in the band gap, electrons may more easily transition from the very bandgap to these specific levels in the central bandgap. As a consequence, the conductivity increases and the band gap decreases [34].

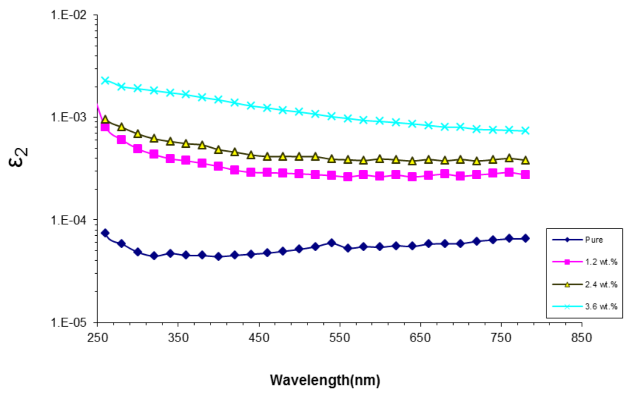

Figure 10. Imaginary dielectric constant for (PEO/PMMA-Co-Ni-Cr Fe_2O_4) nanocomposites films before and after sintering 1200°C with different ferrite ratios

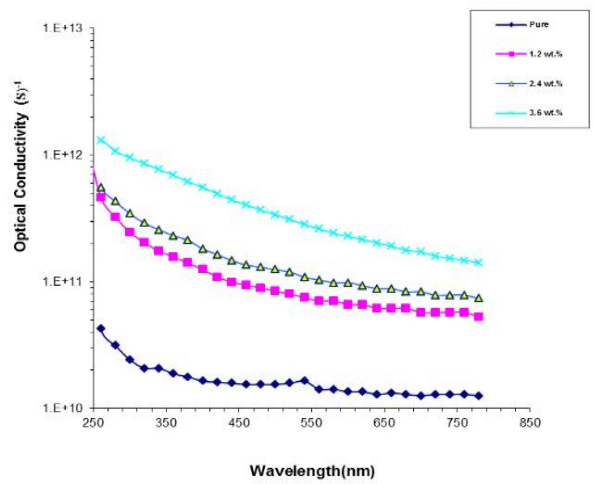

Figure 11. Optical conductivity for (PEO/PMMA-Co-Ni-Cr Fe_2O_4) nanocomposites films 1200°C with different ferrite ratios

Microwave absorption properties:

In order to uncover the characteristics of microwave absorption for (PEO/PMMA-Co-Ni-Cr Fe_2O_4) nanocomposites at 1200°C, the following reflection loss (RL) was calculated using transmission line theory [35, 36]:

$$RL = 20log\left|\frac{Z_{in} - 1}{Z_{in} + 1}\right| \tag{11}$$

$$Z_{in} = \sqrt{\frac{\mu r}{\varepsilon r}} tanh\left[j\left(\frac{2\pi f d}{c}\right)\sqrt{\mu r \varepsilon r}\right] \tag{12}$$

The following formula provides the normalized input impedance (Z_{in}).

$\varepsilon_r = \varepsilon' - j\varepsilon''$, $\mu_r = \mu' - j\mu''$, d is the absorber's thickness in meters, c is the velocity of light in meters per second, and f is microwave frequency in hertz.

At a sample thickness of 50 μm, the RL of various weight fractions of PEO/PMMA-Co-Ni-Cr Fe_2O_4 nanocomposites was measured [37, 38]. Here, a different weight fraction of Co-Ni-Cr Fe_2O_4 is used to compare the reflection loss of PEO/PMMA-Co-Ni-Cr Fe_2O_4 nanocomposites. A minimum RL of -22.8 dB at 11.5 GHz for 3.6 wt% at sintering 1200°C is then displayed in Figure 12 of the PEO/PMMA-Co-Ni-Cr Fe_2O_4 nanocomposite [39, 40]. The following explanation explains why the PEO/PMMA-Co-Ni-Cr Fe_2O_4 composite's microwave absorption improved as the Co-Ni-Cr Fe_2O_4 content rose.

Complex permeability and permittivity are efficiently increased by increasing the Co-Ni-Cr Fe_2O_4 nanocomposite content [39], which produces dielectric/magnetic loss capabilities and matched characteristic impedances [41].

As mentioned, PEO/PMMA-Co-Ni-Cr Fe_2O_4 nanocomposites are promising for a range of technological applications due to their large absorbing bandwidths, lightweight nature, and excellent reflection loss [42].

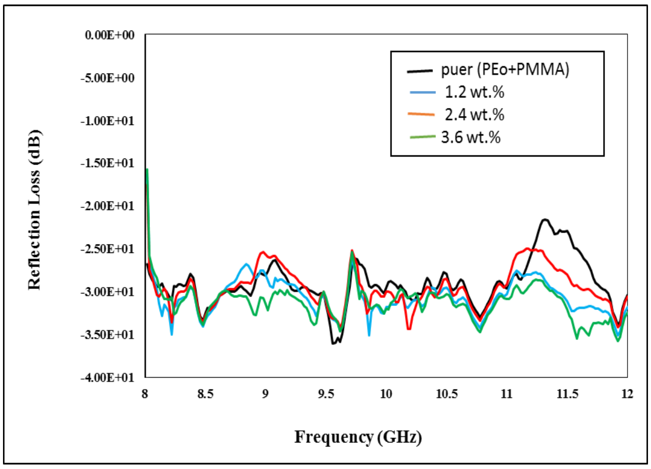

Figure 12. Reflection loss curves for PEO/PMMA-Co-Ni-Cr Fe_2O_4 nanocomposite after sintering at 1200°C with different weight fractions of Co-Ni-Cr Fe_2O_4 in the frequency range 8–12 GHz at the thickness of 50 μm

4. CONCLUSIONS

Nanoparticles of (Co-Ni-Cr Fe_2O_4) were effectively included using the solution-casting technique. Under the light of an optical microscope, the polymers' nanoparticles appear as a seamless network. Charging carriers are able to traverse this network, which is comprised of channels inside nanocomposites. The optical properties showed that the absorption, extinction coefficient, refractive index, real and imaginary dielectric constants, optical conductivity, transmittance, and optical energy gap all rose with increasing nanoparticle concentrations of (Co-Ni-Cr Fe_2O_4). Nanostructures of (Co-Ni-Cr Fe_2O_4) showed promise as a material for optoelectronic devices based on their optical properties. Potential applications for the electromagnetic functionalized synthesized PEO/PMMA-ferrite nanocomposites include materials that absorb microwaves.

REFERENCES

[1] Habeeb, M.A., Hamza, L.A. (2017). Structural, optical and DC electrical properties of (PVA-PVP-Y2O3) films and their application for humidity sensor. Journal of Advanced Physics, 6(1): 1-9. https://doi.org/10.1166/jap.2017.1303

[2] Aid Kazim, B., Al-Nesrawy, S.H. (2023). Thickness influence on the optical properties of (PMMA-PbO) nanocomposites. Journal of Nanostructures, 13(4): 1031-1039. https://doi.org/10.22052/JNS.2023.04.012

[3] Mohammed, A.J., Sameer, H. (2022). Nano ferrite incorporated poly (Vinyl Pyrrolidone (PVP)/Poly (Vinyl Alcohol (PVA) blend: Preparation and investigation of structural, morphological and optical properties. NeuroQuantology, 20(3): 251-258. https://doi.org/10.14704/nq.2022.20.3.NQ22087

[4] Al-Nesrawy, S.H., Awad, N.M., Al-Mamoori, A.Y., Al-Issawe, J.M., Al-Maamori, M.H. (2020). Structural and magnetic properties of magnetic spinel ferrit e (CuxMg1 xFe2O4) 0.0≤X≤0.9 nano-particles. The Mattingly Publishing Co., Inc., 83: 12864-12873.

[5] Hamza, L.A., Muneer, R.M., Hamza, S.A., Khalid, M. (2023). The dielectric properties of (PVA-PVP-Y2O3) nanocomposites. In AIP Conference Proceedings, Baghdad, Iraq, p. 090040. https://doi.org/10.1063/5.0163353

[6] Modi, V.K., Shrives, Y., Sharma, C., Sen, P.K., Bohidar, S.K. (2014). Review on green polymer nanocomposite and their applications. Preservation, 3(11): 17651-17656. https://doi.org/10.15680/IJIRSET.2014.0311079

[7] Abid, A.A., Al-Nesrawy, S.H., Abdulridha, A.R. (2021). New fabrication (PVA-PVP-C. B) nanocomposites: Structural and electrical properties. In Journal of Physics: Conference Series, Iraq, p. 012037. https://doi:10.1088/1742-6596/1804/1/012037

[8] Zafar, M.S. (2020). Prosthodontic applications of polymethyl methacrylate (PMMA): An update. Polymers, 12(10): 2299. https://doi.org/10.3390/polym12102299

[9] Alsaad, A.M., Ahmad, A.A., Qattan, I.A., El-Ali, A.R., Fawares, S.A.A., Al-Bataineh, Q.M. (2021). Synthesis of optically tunable and thermally stable PMMA–PVA/CuO NPs hybrid nanocomposite thin films. Polymers, 13(11): 1715. https://doi.org/10.3390/polym13111715

[10] Dhatarwal, P., Choudhary, S., Sengwa, R.J. (2018). Electrochemical performance of Li+-ion conducting solid polymer electrolytes based on PEO–PMMA blend matrix incorporated with various inorganic nanoparticles for the lithium ion batteries. Composites Communications, 10: 11-17. https://doi.org/10.1016/j.coco.2018.05.004

[11] Abu Hassan Shaari, H., Ramli, M.M., Mohtar, M.N., Abdul Rahman, N., Ahmad, A. (2021). Synthesis and conductivity studies of poly(Methyl Methacrylate) (PMMA) by co-polymerization and blending with polyaniline (PANi). Polymers, 13(12): 1939. https://doi.org/10.3390/polym13121939

[12] Akbari, A., Divband, B., Dehghan, P., Moradi, A.H. (2021). Application of nanocomposites based on graphene and metal materials in measurement of nitrate/nitrite in food samples. Biointerface Research in Applied Chemistry, 11(5): 12769-12783. https://doi.org/10.33263/BRIAC115.1276912783

[13] Reddy, M.R., Subrahmanyam, A.R., Reddy, M.M., Kumar, J.S., Kamalaker, V., Reddy, M.J. (2016). X-RD, SEM, FT-IR, DSC studies of polymer blend films of PMMA and PEO. Materials Today: Proceedings, 3(10): 3713-3718. https://doi.org/10.1016/j.matpr.2016.11.018

[14] Abutalib, M.M., Rajeh, A. (2020). Influence of Fe3O4 nanoparticles on the optical, magnetic and electrical properties of PMMA/PEO composites: Combined FT-IR/DFT for electrochemical applications. Journal of Organometallic Chemistry, 920: 121348. https://doi.org/10.1016/j.jorganchem.2020.121348

[15] ASTM International. (2018). ASTM D882-18: Standard test method for tensile properties of thin plastic sheeting. ASTM International. https://doi.org/10.1520/D0882-18

[16] ASTM International. (2013). ASTM D6988: Standard guide for determination of thickness of plastic film test specimens. West Conshohocken, PA: ASTM.

[17] Nyangasi, L., Andala, D., Onindo, C., Wanyonyi, A., Chepngetich, J. (2018). Processing parameters for electrospinning poly (methyl methacrylate) (PMMA)/titanium isopropoxide composite in a pump-free setup. AAS Open Research, 1: 27. https://doi.org/10.12688/aasopenres.12909.1

[18] Sundaramahalingam, K., Vanitha, D., Nallamuthu, N., Manikandan, A., Muthuvinayagam, M.J.P.B.C.M. (2019). Electrical properties of lithium bromide poly ethylene oxide/poly vinyl pyrrolidone polymer blend elctrolyte. Physica B: Condensed Matter, 553: 120-126. https://doi.org/10.1016/j.physb.2018.10.040

[19] Costa, L.C., Valente, M., Sa, M.A., Henry, F. (2006). Electrical and magnetic properties of Polystyrene doped with Iron nanoparticles. Polymer Bulletin, 57(6): 881-887. https://doi.org/10.1007/s00289-006-0648-6

[20] Hayder, N., Habeeb, M., Hashim, A. (2019). Structural, optical and dielectric properties of (PS-In2O3/ZnCoFe2O4) nanocomposites. Egyptian Journal of Chemistry, 62: 577-592. https://doi.org/10.21608/ejchem.2019.14646.1887

[21] Habeeb, M.A., Kadhim, W.K. (2014). Study the optical properties of (PVA-PVAC-Ti) nanocomposites. Journal of Engineering and Applied Sciences, 9(4): 109. https://makhillpublications.co/files/published-files/mak-jeas/2014/4-109-113.pdf.

[22] Shankar, S., Thakur, O.P., Jayasimhadri, M. (2019). Conductivity behavior and impedance studies in BaTiO3–CoFe2O4 magnetoelectric composites. Materials Chemistry and Physics, 234: 110-121. https://doi.org/10.1016/j.matchemphys.2019.05.095

[23] Martínez-Pérez, J.P., Bolarín-Miró, A.M., Cortés-Escobedo, C.A., Ramírez-Cardona, M., Sánchez-De Jesús, F. (2021). Magnetodielectric study of BiFeO3 synthesized by assisted high-energy ball milling. Journal of Physics and Chemistry of Solids, 153: 109998. https://doi.org/10.1016/j.jpcs.2021.109998

[24] Guzu, A., Ciomaga, C.E., Airimioaei, M., Padurariu, L., et al. (2019). Functional properties of randomly mixed and layered BaTiO3-CoFe2O4 ceramic composites close to the percolation limit. Journal of Alloys and Compounds, 796: 55-64. https://doi.org/10.1016/j.jallcom.2019.05.068

[25] Gupta, B., Agarwal, R., Sarwar Alam, M. (2014). Antimicrobial and release study of drug loaded PVA/PEO/CMC wound dressings. Journal of Materials Science: Materials in Medicine, 25(6): 1613-1622. https://doi.org/10.1007/s10856-014-5184-6

[26] El Fewaty, N.H., El Sayed, A.M., Hafez, R.S. (2016). Synthesis, structural and optical properties of tin oxide nanoparticles and its CMC/PEG–PVA nanocomposite films. Polymer Science Series A, 58(6): 1004-1016. https://doi.org/10.1134/S0965545X16060055

[27] Zhang, X., Wei, S., Haldolaarachchige, N., Colorado, H. A., Luo, Z., Young, D.P., Guo, Z. (2012). Magnetoresistive conductive polyaniline–barium titanate nanocomposites with negative permittivity. The Journal of Physical Chemistry C, 116(29): 15731-15740. https://doi.org/10.1021/jp303226u

[28] Phan, T.T.M., Chu, N.C., Xuan, H.N., Pham, D.T., Martin, I., Carriere, P. (2016). Enhancement of polarization property of silane-modified BaTiO3 nanoparticles and its effect in increasing dielectric property of epoxy/BaTiO3 nanocomposites. Journal of Science: Advanced Materials and Devices, 1(1): 90-97. https://doi.org/10.1016/j.jsamd.2016.04.005

[29] Wu, X., Chen, Z., Cui, Z. (2013). Low temperature synthesis of cubic BaTiO3 nanoparticles. In the 8th Annual IEEE International Conference on Nano/Micro Engineered and Molecular Systems, Suzhou, pp. 399-402. https://doi.org/10.1109/NEMS.2013.6559759

[30] Qi, J., Li, Y., Zhang, X., Wang, J., et al. (2020). Solid-state synthesis semiconducting BaTiO3 nanoparticles at low temperature. Materials Chemistry and Physics, 242: 122496. https://doi.org/10.1016/j.matchemphys.2019.122496

[31] Hashim, A., Habeeb, M.A., Hadi, A. (2017). Synthesis of novel polyvinyl alcohol–starch-copper oxide nanocomposites for humidity sensors applications with different temperatures. Sensor Letters, 15(9): 758-761. https://doi.org/10.1166/sl.2017.3876

[32] Lather, S., Gupta, A., Dalal, J., Verma, V., Tripathi, R., Ohlan, A. (2017). Effect of mechanical milling on structural, dielectric and magnetic properties of BaTiO3–Ni0. 5Co0. 5Fe2O4 multiferroic nanocomposites. Ceramics International, 43(3): 3246-3251. https://doi.org/10.1016/j.ceramint.2016.11.152

[33] Grigalaitis, R., Petrović, M.V., Bobić, J.D., Dzunuzovic, A., et al. (2014). Dielectric and magnetic properties of BaTiO3–NiFe2O4 multiferroic composites. Ceramics International, 40(4): 6165-6170. https://doi.org/10.1016/j.ceramint.2013.11.069

[34] Ghorbani, V., Ghanipour, M., Dorranian, D. (2016). Effect of TiO2/Au nanocomposite on the optical properties of PVA film. Optical and Quantum Electronics, 48(1): 61. https://doi.org/10.1007/s11082-015-0335-7

[35] Sharma, A., Mahajan, H., Mohammed, I., Godara, S.K., Sinha, S., Srivastava, A.K. (2023). Effect of sintering temperature on the structural, dielectric, and magnetic properties of garnet-spinel ferrite composites for use in L-Band devices. Materials Performance and Characterization, 12(1): 64-78. https://doi.org/10.1520/MPC20220084

[36] Badry, R., Hegazy, M.A., Yahia, I.S., Elhaes, H., et al. (2022). Enhancing the optical properties of starch/ZnO nanocomposites using graphene oxide. Egyptian Journal of Chemistry, 65(7): 335-342. https://doi.org/10.21608/ejchem.2021.104153.4811

[37] Alias, M.F.A., Taher, B.Y., Naji, I.S., Iqbal, S., et al. (2019). Effect of deposition parameters on the compositional and optical properties of Cu2SnS3 thin films prepared by chemical bath deposition. Chalcogenide Letters, 16(12): 577-586.
[38] Habeeb, M., Hashim, A., Hayder, N. (2019). Structural and optical properties of novel (PS-Cr2O3/ZnCoFe2O4) nanocomposites for UV and microwave shielding. Egyptian Journal of Chemistry, 62: 697-708. http://doi.org/10.21608/ejchem.2019.12439.1774
[39] Shatti, W.A., Abbas, Z.M.A., Khodair, Z.T. (2022). Co-precipitation method for the preparation of Mn-Zn ferrite and study their structural and magnetic properties. Journal of Ovonic Research, 18(4): 473-479. https://doi.org/10.15251/JOR.2022.184.473
[40] Kulshrestha, S., Shrivastava, A.K. (2016). Crystal growth, optical and structural properties of MNA doped L-histidine single crystal. Scholars Research Library Archives of Physics Research, 7: 9-17.
[41] Moslehi, N.M., Molaei, M.J., Aghaei, A. (2021). Electromagnetic wave absorption properties of barium ferrite/reduced graphene oxide nanocomposites. International Journal of Engineering, 34(6): 1505-1513. https://doi: 10.5829/ije.2021.34.06c.14
[42] Zhu, Y.F., Ni, Q.Q., Fu, Y.Q., Natsuki, T. (2013). Synthesis and microwave absorption properties of electromagnetic functionalized Fe3O4–polyaniline hollow sphere nanocomposites produced by electrostatic self-assembly. Journal of Nanoparticle Research, 15(10): 1988. https://doi.org/10.1007/s11051-013-1988-4